

Measurement of glucose metabolism in the occipital lobe and frontal cortex after oral administration of [1-13C] glucose at 9.4 T

Journal of Cerebral Blood Flow & Metabolism
2022, Vol. 42(10) 1890–1904
© The Author(s) 2022



Article reuse guidelines:
sagepub.com/journals-permissions
DOI: 10.1177/0271678X221104540
journals.sagepub.com/home/jcbfm



Theresia Ziegs^{1,2,*} , Johanna Dorst^{1,2,*} , Loreen Ruhm^{1,2}, Nikolai Avdievitch¹ and Anke Henning^{1,3}

Abstract

For the first time, labeling effects after oral intake of [1-13C]glucose are observed in the human brain with pure 1H detection at 9.4 T. Spectral time series were acquired using a short-TE 1H MRS MC-semiLASER (Metabolite Cycling semi Localization by Adiabatic SElective Refocusing) sequence in two voxels of 5.4 mL in the frontal cortex and the occipital lobe. High-quality time-courses of [4-13C]glutamate, [4-13C]glutamine, [3-13C]glutamate + glutamine, [2-13C]glutamate+glutamine and [3-13C]aspartate for individual volunteers and additionally, group-averaged time-courses of labeled and non-labeled brain glucose could be obtained. Using a one-compartment model, mean metabolic rates were calculated for each voxel position: The mean rate of the TCA-cycle (Vtca) value was determined to be 1.36 and 0.93 $\mu\text{mol min}^{-1} \text{g}^{-1}$, the mean rate of glutamine synthesis (Vgln) was calculated to be 0.23 and 0.45 $\mu\text{mol min}^{-1} \text{g}^{-1}$, the mean exchange rate between cytosolic amino acids and mitochondrial Krebs cycle intermediates (Vx) rate was found to be 0.57 and 1.21 $\mu\text{mol min}^{-1} \text{g}^{-1}$ for the occipital lobe and the frontal cortex, respectively. These values were in agreement with previously reported data. Altogether, it can be shown that this most simple technique combining oral administration of [1-13C]Glc with pure 1H MRS acquisition is suitable to measure metabolic rates.

Keywords

Glucose metabolism, glutamatergic metabolism, human brain, proton magnetic resonance spectroscopy, ultra-high field strengths

Received 1 November 2021; Revised 29 April 2022; Accepted 5 May 2022

Introduction

Human brain metabolism can be studied noninvasively using Carbon-13 (¹³C) MR spectroscopy after the administration of ¹³C labeled substrates, e.g. glucose (Glc). By consuming the ¹³C labeled Glc, its ¹³C nuclei are transferred to pyruvate/lactate by the glycolysis and subsequently further downstream to tricarboxylic acid cycle (TCA) intermediates, which convert e.g. to glutamate (Glu) and glutamine (Gln). In the past, the spectral changes induced by the ¹³C label incorporation were mostly observed via two different approaches: direct ¹³C MRS detection^{1–4} or indirect 1H-[¹³C] MRS methods^{4–7} using editing techniques such as POCE.^{8–11} On the basis of the large number of publications on methods and applications in this field, the

reader is referred to respective review articles,^{12–17} which are explaining and discussing i.e. the details of these methods and the choice of different labeled substrates.

¹High-Field MR Center, Max Planck Institute for Biological Cybernetics, Tübingen, Germany

²IMPRS for Cognitive and Systems Neuroscience, Tübingen, Germany

³Advanced Imaging Research Center, University of Texas Southwestern Medical Center, Dallas, Texas, USA

*These authors contributed equally to this work.

Corresponding author:

Theresia Ziegs, Max Planck Institute of Biological Cybernetics, Max-Planck-Ring 11, 72076 Tübingen, Germany.
Email: theresia.ziegs@tuebingen.mpg.de

Instead of using direct or indirect ^{13}C methods to measure metabolic rates, a new technique was invented by Boumezbeur et al. showing the feasibility of using conventional ^1H MRS without a ^{13}C channel.¹⁸ With this method, the incorporation of ^{13}C nuclei is detectable due to heteronuclear scalar coupling of ^1H and ^{13}C : When ^{13}C nuclei are incorporated into metabolites, the respective ^1H MRS signals of ^{12}C -bonded protons decrease and the signals from ^{13}C -bonded protons increase. Using conventional ^1H MRS, several technical challenges of direct and indirect ^{13}C MRS can be avoided as there is no need for special ^{13}C hardware, like broadband amplifiers, multinuclear transmitters, radiofrequency (RF) coils as well as no special ^{13}C sequences are required. In addition, problems of high specific absorption rates in brain tissue associated with heteronuclear decoupling sequences are not an issue for conventional ^1H MRS.¹⁸ These advantages make the ^1H MRS approach attractive for those MR centers without the possibility of ^{13}C hardware and scanner software as is the case on most clinical MR systems. In contrast, conventional ^1H MRS is usable in most MR centers and benefits from broad expertise concerning RF coils and sequences, which enable the application of an optimal set-up for the study aims.

So far, there are only a few other studies using conventional ^1H MRS to measure ^{13}C label incorporation into downstream metabolites in animals.^{19,20} The first applications to humans have been presented only recently. In 2015 An et al.,²¹ in 2017 Bartnik-Olson et al.²² and in 2020 Dehghani et al.²³ applied Boumezbeur's technique in humans. However, they show data from very few metabolites only: An et al. presented spectral data from different time-points only with decreasing [4- ^{12}C]Glu and [4- ^{12}C]Gln resonance signals but no uptake curves; Bartnik-Olson et al. showed temporal Glu signal decrease of patients with epilepsy and controls; and Dehghani et al. showed uptake curves with the percent enrichment for [4- ^{13}C]Glu, [4- ^{13}C]Glx and [3- ^{13}C]Glx.

In the present study, we follow the incorporation of the ^{13}C nuclei into [4- ^{13}C]Glu, [4- ^{13}C]Gln, [3- ^{13}C]Glx, [2- ^{13}C]Glx, and [3- ^{13}C]Asp after oral administration of [1- ^{13}C]Glc for the individual subjects and could additionally achieve the time course of the labeled and unlabeled Glc in the brain averaged across subjects.

In addition, we show the possibility to measure the rate of glutamine synthesis V_{gln}, the rate of the TCA-cycle V_{tca} and the exchange rate between cytosolic amino acids and mitochondrial Krebs cycle intermediates V_x for the group means, which no human study using Boumezbeur's technique did so far.

Methods

Human subjects

In this study, labeling effects after the oral administration of [1- ^{13}C]Glc were measured in two different brain regions on 11 healthy volunteers (5 female, 6 male, mean age 29 ± 2 years). The measurements were done on 9 of the volunteers in a voxel in the frontal cortex and on 7 of them in a voxel placed in the occipital lobe; so, 5 volunteers were scanned twice with 3–13 weeks between the two sessions. Before the measurement started, the volunteers gave their written informed consent according to the local research ethics regulations, the current version of the Declaration of Helsinki, DIN EN ISO 14 155 and were approved by the Institutional Review Board of the University of Tübingen.

[1- ^{13}C]Glc administration

The volunteers fastened for 9 hours overnight before the measurement started. Before and after the scan the blood sugar level was tested with a glucometer (Accu-Check, Roche Diabetes Care GmbH, Mannheim, Germany) to detect possible hypoglycemia after the Glc administration. Hypoglycemia was not encountered for any subject. For each volunteer, a solution containing 0.75 g of [1- ^{13}C]Glc (Aldrich Chemical Company, Miamisburg, Ohio, USA; API for clinical studies) per kilogram body weight was prepared and the subjects drank the Glc solution after the acquisition of the first spectrum with 64 averages (see below for the measurement details).

Data acquisition

All measurements were performed using a 9.4 T whole-body MR scanner (Magnetom, Siemens Healthineers, Erlangen, Germany). A home-built 4-channel surface coil was used for the measurement in the occipital lobe²⁴ as it is described in Dorst et al.²⁵ and an 8-channel Tx/16-channel Rx volume coil in 3-loop surface transmit mode was used for the voxel in the frontal cortex.²⁶ More details about the coil setup can be found in the Supplementary Material and Figure S1.

Sagittal and transversal gradient-echo scout images were acquired for the positioning of the voxel ($15 \times 18 \times 20 \text{ mm}^3 = 5.4 \text{ ml}$) either in the frontal cortex or the occipital lobe; see Figure 1 for the voxel position and corresponding sample spectra. The voxel in the frontal cortex was placed in the gray matter region centered on the interhemispheric fissure. And the occipital voxel was placed in the right hemisphere 0.5–1 cm from the interhemispheric fissure touching the occipital horn of the lateral ventricle in the right upper corner keeping in mind that the voxel should not

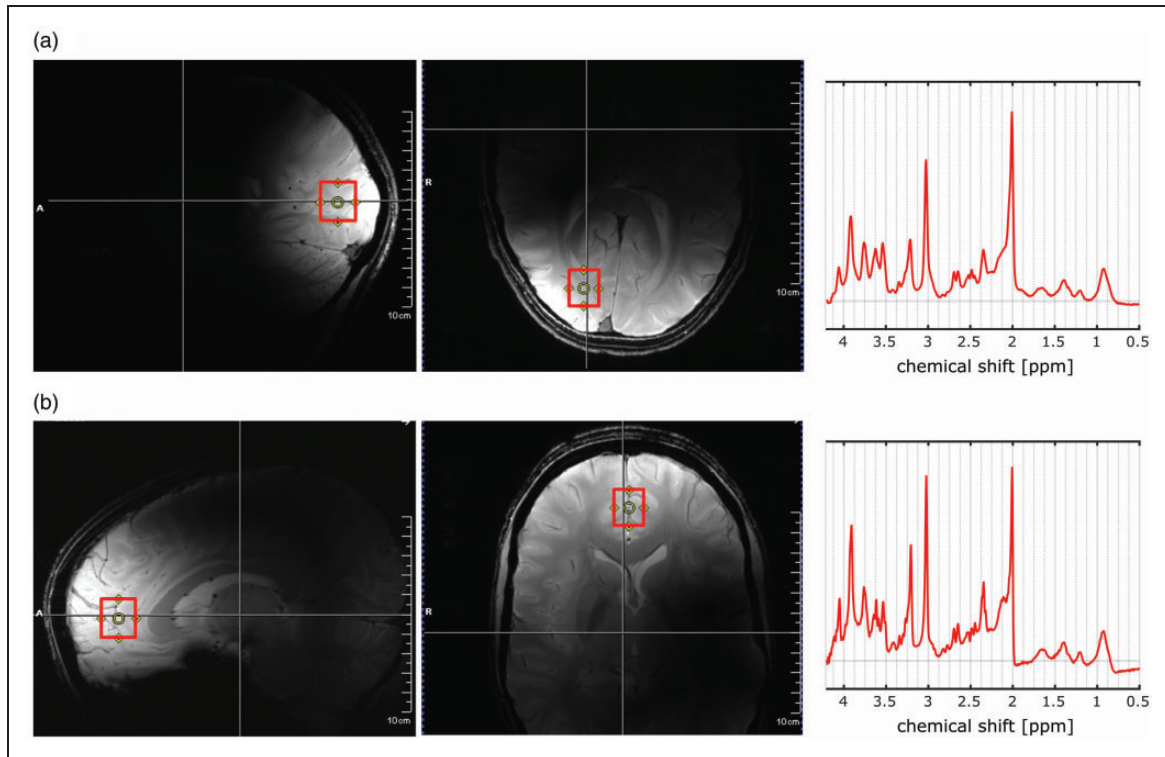


Figure 1. Position of the voxel ($15 \times 18 \times 20 \text{ mm}^2$) in the occipital lobe (a) and the frontal cortex (b) along with the corresponding sample spectra.

be too close to the skull to avoid lipid contamination due to chemical shift displacement error. First-order and second-order B_0 shimming were performed using FAST(EST)MAP,²⁷ and then a voxel-based power calibration was executed.^{28,29} The spectra were measured using a short TE 1H MC-semiLASER sequence; details can be found in Giapitzakis et al.³⁰ with optimizations of the spoiling, phase cycling and crushers later described by Dorst et al.²⁵ (TE/TR = 24/5000 ms, 64 averages (Ave), acquisition time = 512 ms, bandwidth = 8000 Hz, sequence duration = 5.67 min). A water-reference signal (Ave = 16) as well as a macromolecular spectrum^{31,32} (TR = 8 s, Ave = 32) were taken from the same voxel. After the baseline 1H MRS measurement block was executed, the scanner table was pulled out and the volunteers drank the Glc solution as fast as possible (if possible lying flat while drinking with a straw). After the oral intake of [1-13C] Glc, a localizer was applied to verify the position of the voxel. In case of a changed head position the same voxel positioning and calibration procedure were applied as described above including gradient-echo scout sequences to relocate the voxel, B_0 shimming and power calibration before starting the acquisition of a series of MC-semiLASER 1H MRS blocks with 64 averages. The time of repositioning and calibration took 14–21 minutes. If no repositioning of the voxel

was needed, MC-semiLASER blocks of 64 averages were applied immediately after the oral Glc intake. In these cases, the time between Glc intake and start of the data acquisition was 5–9 minutes. In each of the volunteers as many as possible MC-semiLASER 1H MRS blocks of 64 averages were acquired to fill a maximum possible scan time of 2 hours.

Data processing

Raw MRS data were processed with in-house-written code in Matlab (version 2016a; MathWorks, Natick, MA) as described in detail before^{25,30,31,33} and here summarized: (1) replace the data points after 250 ms with zeros; (2) frequency and phase alignment; (3) MC subtraction for the metabolite spectra and the macromolecular data; (4) averaging; (5) eddy current correction using the MC water signal; (6) combine coils using a singular value decomposition method; (7) peak alignment to the NAA signal or the water signal for the water data; (8) removing residual water signal using HSVD for the spectral data; and (9) truncation at 150 ms with subsequent zero filling.

The calculation of the difference spectra needed for the calculation of the metabolite enrichments is explained in the next subsection since extra steps after fitting the pre-Glc-intake spectrum were needed.

Spectral fitting

The ^1H MRS data were fitted with LCModel (V6.3-1L)³⁴ with spectral basis sets simulated with VeSPA (version 0.9.5³⁵) using full quantum mechanical density matrix calculations for the semi-LASER sequence.³⁶ Three separate basis set were generated: for the pre-Glc-intake, for the post-Glc-intake spectra and for the Glc changes in the downfield region.

Pre-Glc-intake basis set. The first basis set was used to analyze the baseline spectra acquired before the oral [1- ^{13}C]Glc intake. The basis set consists of the mean macromolecular spectrum of the volunteers from the occipital lobe (due to lower variability and noise of the data in the occipital lobe than the frontal cortex³⁷) and 13 metabolites: ascorbic acid (Asc), aspartate (Asp), creatine (Cr), γ -aminobutyric acid (GABA), Glc, Gln, Glu, glutathione (GSH), lactate (Lac), myo-inositol (mI), NAA, NAAG, phosphocreatine (PCr), phosphorylethanolamine, scyllo-inositol (scyllo), taurine (Tau), and total choline (tCho, glycerophosphocholine (GPC) + phosphocholine (PCho)). J-coupling constants and chemical shifts were taken from Govindaraju et al.^{38,39} except for the J-coupling constants for GABA, which were taken from Near et al.⁴⁰ The spectra were fitted between 0.6 ppm and 4.2 ppm including water scaling and the LCModel parameter dkntmn (minimum spacing of the spline baseline knots in ppm, cannot exceed one third of the fitted range,⁴¹ which reflects the spline baseline stiffness) was set to 0.25.

Post-Glc-intake basis set. For fitting the changes caused by the incorporation of the ^{13}C nuclei into downstream metabolites, difference spectra were used. No linewidth adjustments were applied. Before subtracting the pre-Glc administration baseline spectrum from the post-Glc administration spectra to obtain a time series of difference spectra, two changes were made: First, the fitted tCr CH_3 peak at ~ 3.0 ppm was subtracted from the pre-Glc spectrum to obtain a pre-Glc spectrum without the tCr CH_3 peak. Thus, the tCr CH_3 will not be subtracted when calculating the difference spectra so that the difference spectra still contained its tCr CH_3 peak, which ensured better LCModel fitting stability since LCModel takes this Cr peak as reference for its first fit iteration. Secondly, the same procedure was used with the upfield Glc peaks: The fitted Glc peaks were subtracted from the pre-Glc spectrum before calculating the difference spectra. The idea behind the second adjustment is the following: the complex multiplets of Glc are often very poorly fitted due to the low concentration and the broad range of chemical shifts between 3.1 ppm–4 ppm. However, the Glc quantification can benefit from the increasing Glc level due to the Glc intake. To keep this advantage, the total Glc level should remain in the difference spectra. Since the unlabeled Glc peaks are indistinguishable for LCModel from the labeled Glc in the upfield region (as seen in Figure 2), the basis set for the post-Glc-intake difference spectra contained the unlabeled Glc metabolite peaks of alpha- and beta-Glc (ratio of 0.36 to 0.64) in addition to the tCr CH_3 peak at ~ 3.0 ppm.

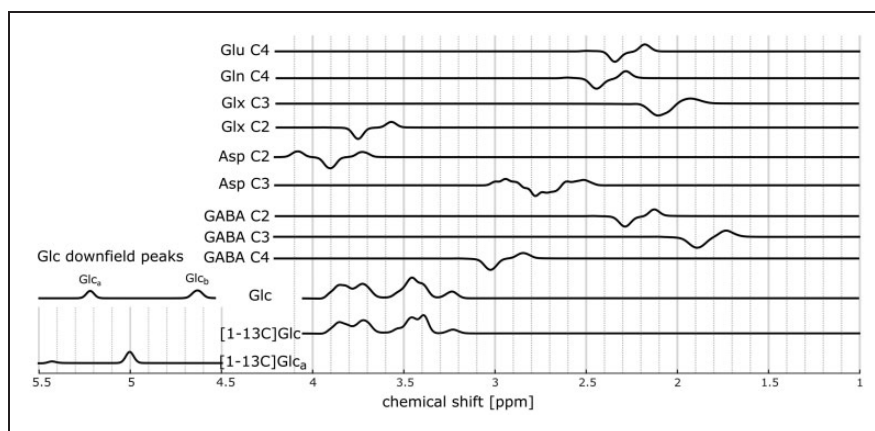


Figure 2. Simulated LCModel basis spectra for metabolites, which are ^{13}C labeled at different carbon positions for the LCModel fit of post-Glc-administration: Glutamate and glutamine labeled at position C4 (Glu C4, Gln C4, respectively), the mix of glutamate and glutamine labeled at position C3 and C2 (Glx C3, Glx C2, respectively), aspartate labeled at position C2 and C3 (Asp C2, Asp C3, respectively) as well as GABA labeled at position C2, C3 and C4 (GABA C2, GABA C3, GABA C4, respectively). These basis spectra were simulated using the method of Boumezbeur et al. as described in the method section to account for the decrease for ^{12}C -bonded protons and the increase of ^{13}C -bonded protons at the same time. In the bottom three rows the unlabeled Glc spectrum for the upfield and the downfield area, the labeled Glc spectrum for the upfield area and the [1- ^{13}C]Glc $_{\alpha}$ were seen for the downfield area. The Glc and the [1- ^{13}C]Glc basis sets are indistinguishable for LCModel. Thus, only the unlabeled Glc basis set was used in the LCModel fits.

Furthermore, the LCMoel basis set for the post-Glc intake difference spectra contained metabolite peaks of Glu, Gln, Asp, Lac, and GABA, which were expected to change after the ^{13}C incorporation with the heteronuclear J-coupling constants taken from de Graaf.⁴² Which metabolites are labeled by the incorporation of the ^{13}C nuclei after [1- ^{13}C]Glc intake is illustrated in previous publications.^{12,43,44} To account for the advantage to simultaneously detect the signal of ^{12}C -bonded and ^{13}C -bonded protons, a method described in Boumezbeur et al.¹⁸ was used, who fitted the difference spectra and combined the corresponding ^{13}C uptake and ^{12}C decrease in one basis set. The method shall be described shortly through the example of Glu labeled at the C4 position:

- If the C4 position of Glu is labeled, the ^{13}C nucleus couples to the 4H-Glu protons at 2.34 and 2.35 ppm with 126.7 Hz. Glu spin systems with and without ^{13}C at the C4 position were simulated with VeSPA. Both simulations were subsequently subtracted to account for the decrease of the unlabeled C4 peak and the increase of the labeled C4 peaks. The basis spectrum was called Glu C4.
- This was done for Gln labeled at the position C4 (Gln C4), for the mix of Glu and Gln labeled at C3 and C2 (Glx C3 and Glx C2, respectively), for GABA labeled at C2, C3 and C4 (GABA C2, GABA C3 and GABA C4), Lac labeled at C3 (Lac C3) and Asp labeled at C2 and C3 (Asp C2 and Asp C3). The simulated basis spectra are shown in Figure 2. Since Lac changes could not be seen in any volunteer, the Lac C3 spectrum was not included in Figure 2. Glu and Gln at the C3 and C2 positions were combined to Glx since the chemical shifts significantly overlap and cannot be distinguished at 9.4 T.

Additionally, the Cho CH_3 peak at ~ 3.2 ppm and the NAA CH_3 peak at 2.0 ppm were added to the basis set to account for subtraction errors, which are mainly caused by the repositioning of the volunteer after the Glc intake. The spectra were fitted between 0.6 ppm and 4.2 ppm including water scaling and the LCMoel parameter dkntmn was set to 999, which is a stiff baseline.

Post-Glc-intake Glc enrichment basis set. Since the fit of the post-Glc-intake difference spectra (previous paragraph) provided only information of the total Glc (Glc_{tot}) concentration, an alternative had to be found to obtain the time-courses for the labeled Glc. So, a closer look has to be taken at the downfield region: While the [1- ^{12}C]Glc $_{\beta}$ peak at 4.630 ppm is overlaid by the water resonance, the decrease in the [1- ^{12}C]Glc $_{\alpha}$ peak at 5.216 ppm is generally detectable.

Unfortunately, the increase of the corresponding [1- ^{13}C]Glc $_{\alpha}$ peaks at 5 and 5.43 ppm could not be reliably detected since the first peak is too close to the water signal, and the second peak is overlaid by an artifact, see Figure 2 for the simulated Glc downfield basis set and Figure S2 for an example of the artifact. Therefore, the post-Glc-intake spectra were fitted with an increased ppm range from 5.1 to 6.2 ppm. In addition, to all metabolites used in the pre-Glc fit, the [1- ^{12}C]Glc $_{\alpha}$ peak at 5.216 ppm and all corresponding ^{13}C labeled metabolites were included in the basis set. Only the fitted values for the [1- ^{12}C]Glc $_{\alpha}$ peak were taken into account for further calculations. The resulting time course for the [1- ^{12}C]Glc $_{\alpha}$ concentration was too variable for single volunteers and thus, the concentrations were averaged across subjects for each position and subsequently fitted with an exponentially decaying function. From the mean time course of Glc_{tot} obtained from the difference spectra and exponential fit of the time course of [1- ^{12}C]Glc $_{\alpha}$ from the downfield fits, the time course of the [1- ^{13}C]Glc can be calculated as follows: Since Glc_{tot} is the sum of [1- ^{13}C]Glc and [1- ^{12}C]Glc, and the level of [1- ^{12}C]Glc can be calculated by [1- ^{12}C]Glc = [1- ^{12}C]Glc $_{\alpha}$ /0.36, the following equation is obtained and used for the calculation of the [1- ^{13}C]Glc enrichment: [1- ^{13}C]Glc = $\text{Glc}_{\text{tot}} - [1-^{12}\text{C}]Glc_{\alpha}/0.36$.

Quantification

Percent Enrichments (PE) of labeled Glu, Gln and Asp were calculated by dividing the concentration of the labeled metabolite of the post-Glc-intake spectra by the concentration of the non-labeled metabolite of the pre-Glc-intake spectrum for each volunteer separately. For metabolic rate calculations, the PEs were averaged across subjects for both voxel positions. The percent enrichment of the [1- ^{13}C]Glc was determined from the time courses of Glc_{tot} from the upfield difference spectra and the time course obtained by the exponential fit of the downfield [1- ^{12}C]Glc $_{\alpha}$ peak changes at ~ 5.2 ppm with the following equation: [1- ^{13}C]Glc/ $\text{Glc}_{\text{tot}} = 1 - [1-^{13}\text{C}]Glc_{\alpha}/0.36/\text{Glc}_{\text{tot}}$.

Metabolic rate determination

The metabolic rates were calculated using the Matlab-based program CWAVE (Version 3.6) from Graeme F. Mason.⁴⁵ This program provides a graphic interface to describe the mass and isotopic flows from the labeled substrate for an arbitrary metabolic model. The program thus solves the differential equations numerically with a 4th/5th order Runge-Kutta¹⁰ algorithm, calculates corresponding metabolic rates of the model and statistical distributions of uncertainties using Monte-Carlo analysis. In this study, a simple

one-compartment model was used describing the incorporation of ^{13}C nuclei from the 1st carbon position of Glc into Glu and Gln at the 4th carbon position and subsequently into Glu and Gln at the 3rd carbon position. The time course of $[1-^{13}\text{C}]\text{Glc}$ is used as the input function, see previous publications^{12,43,44} for illustrations of the labeling pathways. The model (adapted from^{2,46,47}) and the corresponding differential equations can be found in Supplementary Figure S3 and Supplementary Table T1. The one-compartment model was used with the fewest assumptions possible to avoid overfitting and to have a robust estimate of the resulting rates. The present results were compared to the previous literature. Thus, the rate of the TCA-cycle V_{tca} , glutamine synthesis V_{gln} and the exchange rate between cytosolic amino acids and mitochondrial Krebs cycle intermediates V_{x} could be determined for the mean time courses for both voxel positions.

Results

Time series of spectra from two volunteers from the occipital lobe and the frontal cortex are shown in Figure 3(a) and (b). Most dominant is the labeling effect in the region between 2 and 2.5 ppm: the $[4-^{12}\text{C}]\text{Glu}$ peak at ~ 2.34 ppm decreases and the $[4-^{13}\text{C}]\text{Glu}$ peaks at 2.18 and 2.5 ppm increase. The same is seen for the $[4-^{12}\text{C}]\text{Gln}$ peak at ~ 2.44 ppm and the corresponding $[4-^{13}\text{C}]\text{Gln}$ satellite peaks. The zoomed part of Figure 3 makes these spectral pattern changes better visible by a selection of spectra from six time points with color coding of frequency ranges corresponding to the Glu and Gln peaks in yellow and red, respectively.

The summation of all volunteers' difference spectra between the respective first and last acquired spectra for both voxel positions in Figure 3(c) reveals changes due to the labeling at the 4th Glu and Gln carbon position, the 3rd Glx and Asp carbon position and the 2nd Glx and Asp carbon position. The changes of $[3-^{13}\text{C}]\text{Lac}$ were minor. Metabolite peaks with increasing amplitude are marked in green and those with decreasing amplitude are indicated in blue. Additionally, subtraction errors are seen at the tCr CH_3 peak at 3.0 ppm, the tCho CH_3 peak at ~ 3.2 ppm and the NAA CH_3 peak at 2.0 ppm. The region from 3.8 to 4.2 ppm shows artifacts and thus cannot be interpreted.

The difference spectra, the fitted metabolite spectra and the fit residual for different time points are shown for one sample volunteer in Figure 4; colors indicate different time points. The increase of the (negative) ^{12}C peaks and the (positive) ^{13}C satellite peaks are clearly detectable.

In general, the data quality is better in the occipital lobe than the frontal cortex in terms of SNR and

variability between time points, due to the high receive SNR surface coil specifically made for SVS in the occipital lobe and higher impact of motion in the frontal cortex. See Supplementary Material and Supplementary Figure S4 and S5 for more details about FWHM and SNR of the measurements in both voxel positions.

Mean time courses for the total, labeled and unlabeled Glc are shown in the first row of Figure 5(a). The data from the single volunteers are summarized in boxplots in Supplementary Figure S6. The Cramér-Rao-Lower-Bound (CRLB) for the fitted Glc_{tot} , calculated from LCMoDel, was $4 \pm 2\%$ and $11 \pm 6\%$ (mean \pm std across subjects) for the measurements of the occipital lobe and the frontal cortex, respectively. The time courses of $[4-^{13}\text{C}]\text{Glu}$, $[4-^{13}\text{C}]\text{Gln}$, $[3-^{13}\text{C}]\text{Asp}$, $[3-^{13}\text{C}]\text{Glx}$, $[2-^{13}\text{C}]\text{Glx}$ for each volunteer are summarized in boxplots for the occipital lobe (black, 1st column) and the frontal cortex (red, 2nd column), see 2nd row and the following of Figure 5. The third column of Figure 5 presents the percent enrichment (PE) calculated from the mean concentration for both voxel positions. The maximum enrichment of the brain Glc was 58.5% and 54.8% for the occipital lobe and frontal cortex, respectively. For the other metabolites, the following enrichments were achieved after 2 h of measurement: $[4-^{13}\text{C}]\text{Glu}$: 24% and 24%, $[4-^{13}\text{C}]\text{Gln}$: 15% and 20%, $[3-^{13}\text{C}]\text{Asp}$: 41% and 37%, $[3-^{13}\text{C}]\text{Glx}$: 19% and 17%; $[2-^{13}\text{C}]\text{Glx}$: 19% and 23% for the occipital lobe and frontal cortex, respectively.

For the calculation of the mean concentration as well as the PE, those data were removed, where the fit of the metabolite is zero for more than half of the time points or show clearly incorrect time courses, which strongly differ from the median.

The rates V_{gln} , V_{tca} and V_{x} were calculated for both measured positions and are shown in Table 1 including the results of the Monte-Carlo error analysis from CWave. In Figure 6, the respective data and fitted curves from CWave are seen for $[4-^{13}\text{C}]\text{Glu}$, $[4-^{13}\text{C}]\text{Gln}$ and $[3-^{13}\text{C}]\text{Glx}$.

Discussion

In this study, effects of ^{13}C labeling in ^1H MR spectra from two voxel positions in healthy human brain after oral intake of $[1-^{13}\text{C}]\text{Glc}$ were presented acquired with an MC-semiLASER sequence at 9.4T. Using a pure ^1H MRS technique without the presence of any ^{13}C hardware, as introduced by Boumezbeur et al.,¹⁸ uptake curves for a larger number of metabolites could be obtained than before with this approach: temporal data from labeled and unlabeled Glc, $[4-^{13}\text{C}]\text{Glu}$, $[4-^{13}\text{C}]\text{Gln}$, $[3-^{13}\text{C}]\text{Asp}$, $[3-^{13}\text{C}]\text{Glx}$ and $[2-^{13}\text{C}]\text{Glx}$ are shown herein. The data quality of the averaged

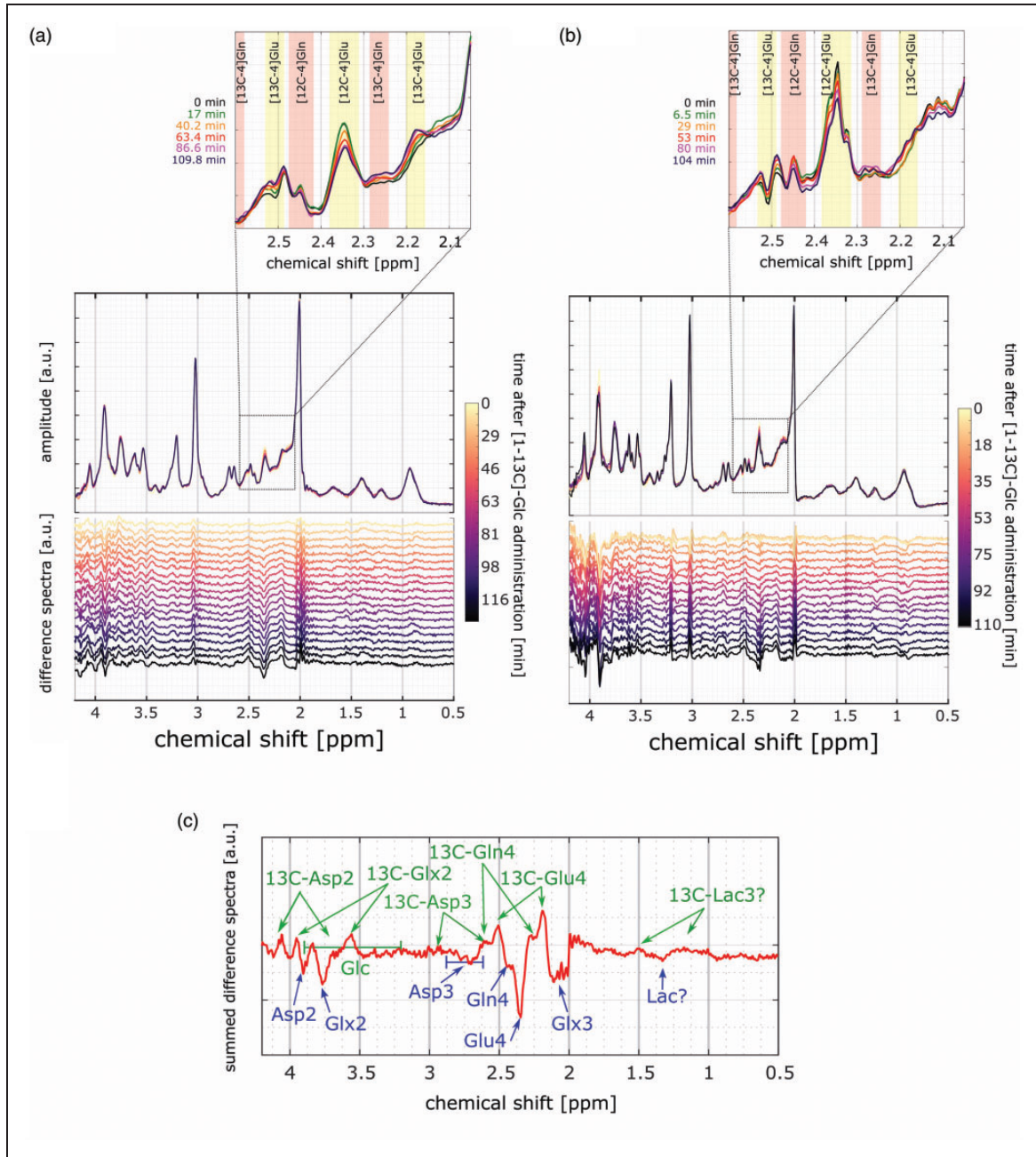


Figure 3. Time series of spectra and difference spectra from (a) occipital lobe and (b) frontal cortex. The changes for the ^{12}C -bonded H4-glutamate and -glutamine signals are highlighted in the zoomed figure above for a few selected time points. (c) Sum of the last difference spectrum for all volunteers. Decreasing metabolite peaks with ^{12}C -bonded protons are marked in blue and increasing satellite peaks due to the coupling to ^{13}C are marked in green. In the lower panel, subtraction errors at the NAA $^2\text{CH}_3$, Cr CH_3 and Cho CH_3 peaks are additionally shown.

time course across subjects was sufficient to obtain rate estimates for the TCA cycle rate V_{tca} , the glutamine synthesis rate V_{gln} and the exchange rate of TCA cycle intermediates with cytosolic amino acids V_x , which are in agreement with literature values. None of the previous human studies using a pure ^1H MRS technique

calculated these rates and only two animal studies presented data for V_{tca} .^{18,20}

Oral administration

So far, the infusion of ^{13}C labeled substrates was common to investigate brain metabolism and only

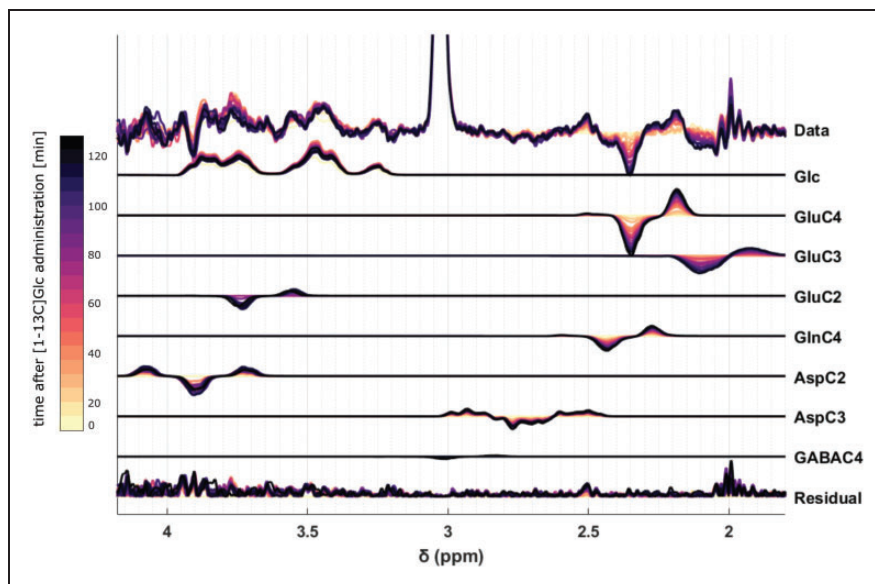


Figure 4. Difference spectra and fitted metabolite basis sets for the metabolites of interests with the remaining Cr CH₃ peak at 3 ppm. In addition, the residual of the difference spectra and the fit are displayed. Sample data from one volunteer from the occipital lobe. Colors indicate time points from light to dark (yellow for short after the Glc intake to black at the very end of the measurement).

a few studies used an oral administration: One used an oral intake exclusively⁴⁸ and three other studies compared infusion and oral protocols.^{1,4,49} Both administrations have certain advantages and disadvantages, which will be discussed below:

1. One downside of the oral intake is the delayed labeling of the metabolites due to the gastrointestinal Glc absorption, which is avoided by intravenous (i.v.) administration. The delay leads to prolonged examination times^{1,4} and thus potentially in increasing motion artifacts and scan time costs.
2. Secondly, a larger percentage of Glc retained in liver⁵⁰ results in a higher amount of Glc needed in an oral protocol than in i.v. administration to reach similar enrichment levels. Moreno et al.⁴⁹ showed that comparable results are achieved in a low dose infusion protocol with only 1/3 of the Glc amount of an oral dose. On the other hand, the costs per gram ¹³C labeled Glc approved for i.v. administration might be significantly higher than the costs for Glc applicable for oral intake due to the need for a higher clinical trial grade and tests from a specialized pharmacy guaranteeing the safety of the i.v. administration. Furthermore, with an oral intake the effort of the study set-up and the associated costs for additional material (i.v. pumps, i.v. lines, Teflon needles etc.) and people (phlebotomist/doctor/nurse) are largely reduced.
3. While oral and i.v. administration lead to similar mean rates of Vtca and Vgln, Mason et al.⁴ objects

that the oral intake leads to a several-fold bigger standard deviation (SD). In contrast to the i.v. set-up, where the bolus infusion leads to a quick Glc PE increase, the oral intake results in a delayed Glc enrichment, see point 1 above, and thus, the uptake curve of Glc PE resemble the time courses of the consequently labeled metabolites more. As a consequence, the simulated curves become less sensitive to the rate constants,⁴ which requires higher precision and accuracy of these time courses than in an i.v. protocol. Nonetheless, Mason et al. worked out that the major part of the uncertainty in an oral set-up in comparison to an i.v. administration is caused by imprecise knowledge about the kinetics of the glucose arrival in the brain. As most studies determine the brain Glc PE from the blood Glc PE, the limiting factors are: uncertainties of sampling time (length of the i.v. line) and differences between enrichment of the arterial blood Glc in the brain and venous plasma Glc sampling location.⁴ This reason could partly be solved by measuring the Glc enrichment directly in vivo in the brain, which is generally possible as Pfeuffer et al.⁵¹ showed in rat brain at 9.4 T using a ¹H-[¹³C]MRS. Unfortunately, the individual subject's Glc enrichment could not be obtained in the present study but only group means are reported. To focus on the detection of downfield Glc peaks in humans could be a valid aim for future studies to access individual brain Glc PEs.

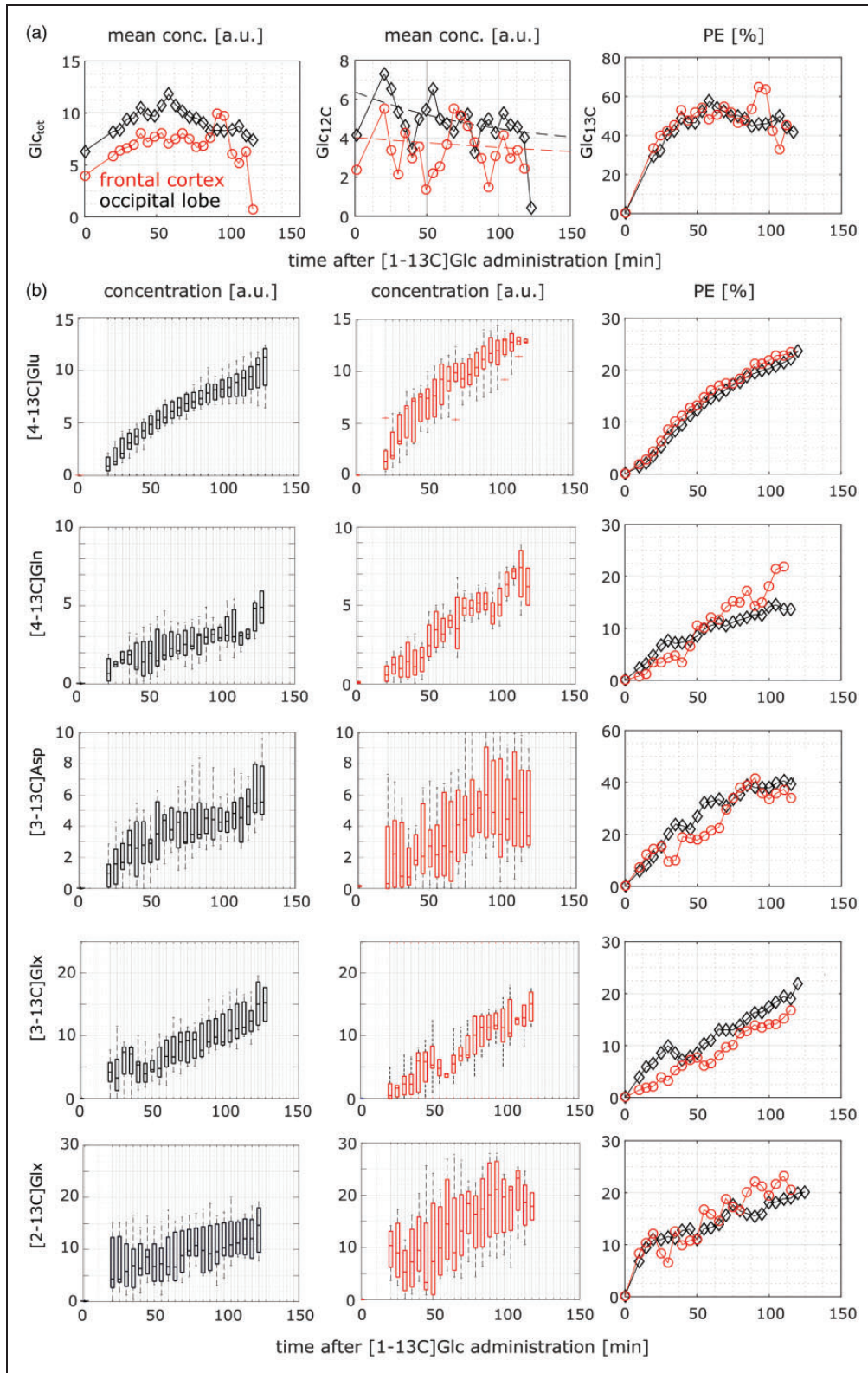


Figure 5. (a) The first row shows mean concentrations across all volunteers in the occipital lobe (black) and frontal cortex (red). The columns show data Glc_{tot}, Glc_{12C} in addition to an exponential fit and Glc_{13C} and In (b) the time courses for different labeled metabolites is shown. The range of concentration for each volunteer for the occipital lobe (first column), frontal cortex (second column) and the percent enrichment (PE) calculated from the mean concentration for each position is presented. For the calculation of the mean concentration as well as the percent enrichment, data from volunteers, which are too far from the median, were removed. See methods section for more information.

Table 1. Calculated rates with a 1-compartment metabolic model using CWave (mean, std): the combined rate of glutamine synthetase and glutaminase V_{Gln} , TCA cycle rate V_{Tca} and the TCA cycle intermediates exchange rate V_{x} .

	V_{Gln} ($\mu\text{mol min}^{-1} \text{g}^{-1}$)	V_{Tca} ($\mu\text{mol min}^{-1} \text{g}^{-1}$)	V_{x} ($\mu\text{mol min}^{-1} \text{g}^{-1}$)
OCC	0.23 ± 0.03	1.36 ± 0.05	0.57 ± 0.05
FRONT	0.45 ± 0.03	0.93 ± 0.04	1.21 ± 0.09

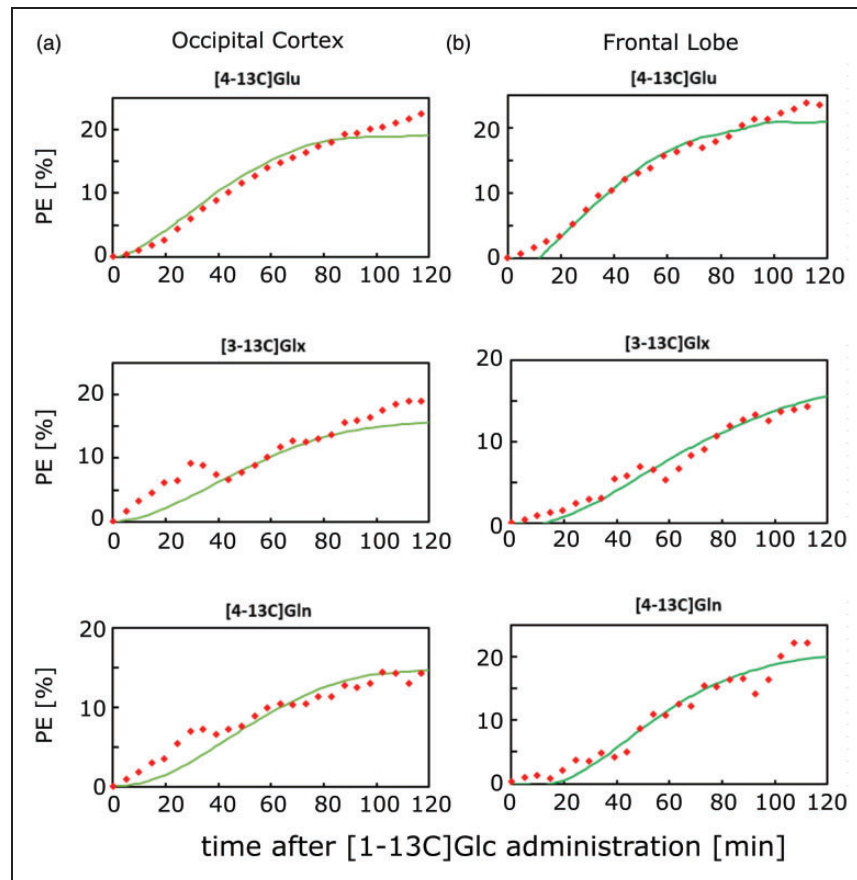


Figure 6. Experimental mean percent enrichment for [4-13C]Glu, [3-13C]Glx and [4-13C]Gln for both voxel positions (red dots) and the fitted curve from CWave (green) with a single-compartment model in (a) for the occipital lobe and in (b) for the frontal cortex.

4. Beside these downsides, the major advantages of oral administration are the reduced effort in the set-up and the significantly higher comfort for the volunteers. This enlarges the pool of potential volunteers and patients to participate in neuroscientific and clinical trials enormously, since many more people are willing to drink a sugar solution, but may refuse a catheterization e.g. in case of needle phobia.

Time courses of labeled metabolites

Most previous studies showing uptake curves in human brain focused on the detection of [4-13C]Glu, [4-13C]Gln, [3-13C]Glu, [3-13C]Gln, or combination of Glu

and Gln.^{3,4,10,22,23,46,52–54} Although some studies could also detect the labeling of additional metabolites in their MR spectra, only a very few studies displayed uptake curves of other metabolites: [2-13C]NAA,⁴³ [2-13C]Glu,^{2,55} [2-13C]Gln,^{2,55} [3-13C]Lac,^{1,56} [2,3-13C]Asp,¹ and [2-13C]Asp.^{43,55,56}

In this study, time courses of a relatively broad range of metabolites could be obtained at once: 13C labeled and 12C unlabeled Glc, [4-13C]Glu, [4-13C]Gln, [3-13C]Asp, [3-13C]Glx, [2-13C]Glx. The time courses of labeled Lac, labeled GABA and [2-13C]Asp could not be achieved. Lactate did not seem to change and the concentration of GABA is too low to detect respective changes.

Glc enrichment. In many cases, the LCModel fit of Glc_{tot} in the upfield region in 1H single voxel spectra even in ultra-high field MRS measurements is incorrect or even unsuccessful.^{29,57} But the Glc_{tot} data of this human brain 9.4T study is of high quality. However, the fit of the $[1-^{12}C]Glc_z$ peak in the downfield region exhibits a high variance, which is why an exponential fit on the mean $[1-^{12}C]Glc_z$ time course across subjects was used to derive the $[1-^{13}C]Glc$ PE.

The shape of the time course of $[1-^{13}C]Glc$ is similar in both voxel positions and resembles the time courses from other oral Glc intake studies.^{49,58} The enrichments in the current study are higher than the value of 38.3% Moreno et al.⁴⁹ reported, but they used 0.65 g/kg body weight, which is 0.1 g/kg body weight Glc less in their oral protocol. Unfortunately, many studies show only the plasma Glc enrichment instead of the brain Glc enrichment. Assuming that the fractional enrichment of plasma and brain Glc is similar,^{9,20,49} both values can be compared: The ^{13}C MRS study from Mason et al.⁴ using the same $[1-^{13}C]Glc$ amount in the oral set-up, showed plasma Glc PE of more than 75%. Most infusion studies report peak values of the brain Glc enrichment of about 60–70% (in animals^{20,59} or humans^{49,60}) which depends on the amount of Glc infused, but the amount of Glc of the maintenance dose after the initial bolus is not reported in most studies. Altogether, the results of this study are in line with previous reports.

Glutamate and glutamine enrichment. The $[4-^{13}C]Glu$ enrichment curves for both voxel positions show good quality time courses with low noise. The concentration of $[4-^{13}C]Glu$ increases faster in the frontal cortex, but both PE curves are fairly the same. The shape of the concentration curves look similar to those reported in previous oral ^{13}C MRS studies:^{4,49} fast increase in the first hour, reduced increase afterwards and Mason et al.⁴ shows that it reaches a saturation plateau after about 3 hours of measurement, which could not be performed in the present study since scan time was restricted to a maximum of 2 hours. A relocation after a break in between as Mason et al. suggested, would add significant uncertainty.

Mason et al.⁴ reported about 20% $[4-^{13}C]Glu$ enrichment for the oral administration with the same Glc amount as used in the present study and the peak enrichment reported by Moreno et al.⁴⁹ was 16% (as already mentioned, they used less Glc). The only study using Boumezbear's technique on humans showing enrichment curves was Dehghani et al.²³ using an infusion protocol leading to approx. 15% PE. Other infusion studies using $[1-^{13}C]Glc$ in humans measured PEs between approx. 17–32%.^{2,3,10,46,55} Many other studies

reported the signal intensity in arbitrary units or the concentration in mmol/kg or mM and no fractional enrichment. It can be concluded, that the herein measured maximum PE for $[4-^{13}C]Glu$ is in the range of previously reported values.

The $[4-^{13}C]Gln$ enrichment values are in line with previous results, although the data from the frontal cortex show high variability, and the final enrichment should be treated with caution: The only oral study presenting $[4-^{13}C]Gln$ concentration curves from Mason et al. indicates a PE of approx. 14–17%.⁴ Previous infusion studies reported a PE of approx. 25%.^{2,46}

There are only a few literature values from human studies and no data from oral experiments to compare the $[3-^{13}C]Glx$ data: Dehghani et al.²³ shows an increase of 5–10% after 1 h using Boumezbear's technique; and other infusion studies determined a labeling of 23% of $[3-^{13}C]Glu$ after 3 h of measurement.^{3,46} These values are comparable to those measured in the present study.

The PE of $[2-^{13}C]Glx$ is also similar to the previously reported values of 10–15% for $[2-^{13}C]Glu$ and $[2-^{13}C]Gln$ ² after 1 h of measurement in an infusion study.

Aspartate enrichment. For the 1H MRS data reported herein, only $[3-^{13}C]Asp$ time courses could be detected. Changes in the $[2-^{13}C]Asp$ peaks could not be successfully quantified due to two reasons: First, the spectral range of the $[2-^{12}C]Asp$ peak at 3.9 ppm is disturbed by an artifact, and secondly, one of the satellites peaks due to the ^{13}C labeling occurs at 4.1 ppm, which is strongly influenced, by residual water signal and corresponding baseline errors. The artifact at 3.9 ppm could also cause the high PE values of $[3-^{13}C]Asp$, if the fitting of Asp in the pre-Glc spectra was underestimated as a consequence. The reference PE values in previous literature are definitely lower than the present values. Two human studies determined PEs of $[2-^{13}C]Asp$ of 12%⁴³ and $[3-^{13}C]Asp$ of 27%.³

Metabolic rate calculations

The $[4-^{13}C]Glu$ curves show the best fit for time points <100 min. The uptake curves for time points >100 min are still rising while the fit is not, which indicates that the input function (labeled Glc) is not correctly determined for >100 min. Other reasons for discrepancies of fitted and experimental time courses can be the incompleteness of the one-compartment model. It does not take the regional/cellular heterogeneity⁴⁷ and the compartmentalization of the metabolites, into account e.g. Glu is higher concentrated in neurons and Gln in glia cells. Consequently, the V_{tca} rate calculated reflects

mostly neuronal metabolism.⁶¹ Since overly sophisticated models come with the risk of overfitting,^{62,63} a more complex analysis with two or even more compartments would have been sensible when individual Glc time-courses would have been accessible in an appropriate quality and additional information could have been obtained such as segmentation of tissue types¹⁰ or alternative labeling schemes. In addition, it would be crucial to evaluate the influence of different assumptions within the model (concentration of TCA intermediates, dilution rates, etc.) on the fitted rate values (as it was partly done in^{47,64}) as well as its robustness. However, such an analysis is beyond the scope of the herein presented study.

Nevertheless, the metabolic rates are in agreement with previous literature: The glutamine synthesis rate V_{Gln} is in the range of the values from oral⁴ and infusion studies.^{2,4,46,52,64} Although V_{Gln} for the frontal cortex is more on the upper limit of the range of rates previously reported. The rate of the TCA cycle in the frontal cortex is similar to previous reports in infusion studies,^{2,10,46,52,65} while the V_{Tca} rate from the occipital lobe is somewhat higher than the highest previously reported values.^{10,65} The rate of the exchange of TCA cycle intermediates with cytosolic amino acids V_{x} in the occipital lobe was found to be the same as in an infusion study⁶⁴ (and animal studies show similar values for V_{x} ^{5,18,47,66}) but the V_{x} rate for the frontal cortex was about twice as high. Previous studies predict a V_{x} rate, which is comparable to V_{Tca} ,^{64,67} but there seems to be still no consensus of the correct V_{x} value.^{16,68}

The SDs of the metabolic rates in Table 1 are rather small although the SNR of the difference spectra for the labeled metabolites is relatively low, see Supplementary Figure S5. The reasons for this apparent discrepancy are the following: CWave's calculation of the SDs depends on the variance of the uptake curves. Their variances are relatively small since they result from averaged individual curves and averaging obviously reduces the variance. Particularly, the important time course of [4-13C]Glu is very smooth, see Figure 5. The second explanation is that the fitting procedure takes full advantage of the present method to simultaneously detect the 12C- and the 13C-bonded proton signals by combining both in one basis spectrum (see subsection Post-Glc-intake basis set). Thus, the uptake curves are more accurate than the SNRs from the difference spectra may indicate, since the SNRs were calculated from the maximal peak change of the metabolites only.

Problems and improvements

Further improvements of the oral study setup can be achieved with the use of [1,6-13C]Glc or [U-13C]Glc,

which doubles the sensitivity since two pyruvate molecules can be labeled instead of only one pyruvate molecule from [1-13C]Glc. On the other hand, [1,6-13C]Glc costs about 5 times more than [1-13C]Glc (which was already approx. 5000 euro/person) and is thus not affordable for human studies. [U-13C]Glc would be a less expensive alternative. It would label additional positions, which should have negligible effects on the 1H spectra.^{15,42,69} For the present study, [U-13C]Glc would have been still more expensive than [1-13C]Glc (approx. twice the price of [1-13C]Glc).

A problem of this study was the break within the scan session to drink the labeled Glc. In most cases, the scanner table was pulled out of the whole-body scanner and the volunteers drank the solution with a straw while lying flat; in a few cases, the volunteers had to come out of the head coil completely to drink the solution sitting. Although no volunteer reported problems with choking in the lying position, the possibility of choking has to be kept in mind. The re-positioning of the post-Glc voxel to the original voxel was not in all cases perfect. Although the voxel position was corrected manually by visual inspection, a small possible mismatch of pre-Glc to post-Glc voxel position remains. A possible solution would be to use automatic voxel positioning as it exists at many clinical scanners, but not for the 9.4 T scanner used in this study.

While time courses of many differently labeled metabolites could be determined for most volunteers individually, the Glc time-course is less accurate and could only be evaluated as a mean of all volunteers for each voxel position. Especially, the time-course of the downfield Glc showed high variance, which would be reduced if the artifact at 5.4 ppm could be avoided, and thus, the increasing [1-13C]Glc_α peak could be evaluated directly. Additionally, the time courses from both labeled Asp positions could potentially be determined without this artifact. Alternatively, individual brain Glc enrichments could be achieved if blood is drawn (which was not possible in the present study inside a non-clinical setting) to obtain individual rate measurements.

A minor uncertainty is caused by the time the volunteers needed for drinking the Glc solution, so the starting time might vary for about one minute.

Conclusion

Oral administration of [1-13C]Glc leads to detectable changes in 1H MRS spectra acquired in the human brain at 9.4 T in the occipital lobe as well as in the frontal cortex. From time courses of labeled and unlabeled Glc, [4-13C]Glu, [4-13C]Gln, [3-13C]Glx, [2-13C]Glx and [3-13C]Asp, the corresponding rates V_{Tca} , V_{Gln} and V_{x} could be calculated for the average

across subjects and are in accordance to literature values. These results support the applicability of oral administration of ^{13}C labeled Glc and conventional ^1H MRS at ultra-high field to assess metabolic turnover rates in the human brain.

Funding

The author(s) disclosed receipt of the following financial support for the research, authorship, and/or publication of this article: The study was funded by SYNAPLAST (Grant No. 679927 to T.Z., J.D., L.R., and A.H.) and Cancer Prevention and Research Institute of Texas (CPRIT) (Grant No. RR180056 to A.H.)

Acknowledgements

We thank Dr Graeme Mason, Yale University, for providing the CWave software.

Declaration of conflicting interests

The author(s) declared no potential conflicts of interest with respect to the research, authorship, and/or publication of this article.

Authors' contributions

Theresia Ziegs contributed to the concept and design of the study; acquired, analyzed and interpreted the data as well as drafted and revised the article. Johanna Dorst programmed and optimized the sequence and developed the measurement set-up. Loreen Ruhm assisted with the acquisition and interpretation of the data. Nikolai Avdievitch designed and built the coil. Anke Henning obtained the funding, supervised the study, and contributed to its concept and design as well as to the interpretation of the data and revising the manuscript.

Availability of data and materials

Data sets, code, and additional information will be provided by the authors upon request.

ORCID iDs

Theresia Ziegs  <https://orcid.org/0000-0002-7847-1713>

Johanna Dorst  <https://orcid.org/0000-0002-2028-6291>

Supplemental material

Supplemental material for this article is available online.

References

- Blüml S, Moreno A, Hwang J-H, et al. ^1H - ^{13}C glucose magnetic resonance spectroscopy of pediatric and adult brain disorders. *NMR Biomed* 2001; 14: 19–32.
- Chhina N, Kuestermann E, Halliday J, et al. Measurement of human tricarboxylic acid cycle rates during visual activation by ^{13}C magnetic resonance spectroscopy. *J Neurosci Res* 2001; 66: 737–746.
- Gruetter R, Novotny EJ, Boulware SD, et al. Localized ^{13}C NMR spectroscopy in the human brain of amino acid labeling from D-[^1H - ^{13}C] glucose. *J Neurochem* 2002; 63: 1377–1385.
- Mason GF, Petersen KF, de Graaf RA, et al. A comparison of ^{13}C NMR measurements of the rates of glutamine synthesis and the tricarboxylic acid cycle during oral and intravenous administration of. *Brain Res Protoc* 2003; 10: 181–190.
- Lanz B, Xin L, Millet P, et al. In vivo quantification of neuro-glial metabolism and glial glutamate concentration using ^1H -[^{13}C] MRS at 4.1T. *J Neurochem* 2014; 128: 125–139.
- Kauppinen RA, Pirttila TRM, Auriola SOK, et al. Compartmentation of cerebral glutamate in situ as detected by $^1\text{H}/^{13}\text{C}$ n.m.r. *Biochem J* 1994; 298: 121–127.
- Kauppinen RA and Williams SR. Nondestructive detection of glutamate by ^1H nuclear magnetic resonance spectroscopy in cortical brain slices from the Guinea pig: Evidence for changes in detectability during severe anoxic insults. *J Neurochem* 1991; 57: 1136–1144.
- Rothman DL, Behar KL, Hetherington HP, et al. ^1H -Observe/ ^{13}C -decouple spectroscopic measurements of lactate and glutamate in the rat brain in vivo. *Proc Natl Acad Sci U S A* 1985; 82: 1633–1637.
- Rothman DL, Novotny HJ, Shulman GI, et al. ^1H -[^{13}C] NMR measurements of [^4H - ^{13}C] glutamate turnover in human brain. *Proc Natl Acad Sci USA* 1992; 89: 9603–9606.
- Mason GF, Pan JW, Chu WJ, et al. Measurement of the tricarboxylic acid cycle rate in human grey and white matter in vivo by ^1H -[^{13}C] magnetic resonance spectroscopy at 4.1T. *J Cereb Blood Flow Metab* 1999; 19: 1179–1188.
- De Feyter HM, Herzog RI, Steensma BR, et al. Selective proton-observed, carbon-edited (selPOCE) MRS method for measurement of glutamate and glutamine ^{13}C -labeling in the human frontal cortex. *Magn Reson Med* 2018; 80: 11–20.
- de Graaf RA, Mason GF, Patel AB, et al. In vivo ^1H -[^{13}C] NMR spectroscopy of cerebral metabolism. *NMR Biomed* 2003; 16: 339–357.
- Morris P and Bachelard H. Reflections on the application of ^{13}C -MRS to research on brain metabolism. *NMR Biomed* 2003; 16: 303–312.
- Rothman DL, Behar KL, Hyder F, et al. In vivo NMR studies of the glutamate neurotransmitter flux and neuroenergetics: implications for brain function. *Annu Rev Physiol* 2003; 65: 401–427.
- de Graaf RA, Rothman DL and Behar KL. State-of-the-Art direct ^{13}C and indirect ^1H -[^{13}C] NMR spectroscopy in vivo: a practical guide. *NMR Biomed* 2011; 24: 958–972.
- Rothman DL, De Feyter HM, de Graaf RA, et al. ^{13}C MRS studies of neuroenergetics and neurotransmitter cycling in humans. *NMR Biomed* 2011; 24: 943–957.
- Rothman DL, de Graaf RA, Hyder F, et al. In vivo ^{13}C and ^1H -[^{13}C] MRS studies of neuroenergetics and neurotransmitter cycling, applications to neurological and psychiatric disease and brain cancer. *NMR Biomed* 2019; 32: 1–21.

18. Boumezbeur F, Besret L, Valette J, et al. NMR measurement of brain oxidative metabolism in monkeys using ^{13}C -labeled glucose without a ^{13}C radiofrequency channel. *Magn Reson Med* 2004; 52: 33–40.
19. Xu S, Yang J and Shen J. Measuring N-acetylaspartate synthesis in vivo using proton magnetic resonance spectroscopy. *J Neurosci Methods* 2008; 172: 8–12.
20. Valette J, Boumezbeur F, Hantraye P, et al. Simplified ^{13}C metabolic modeling for simplified measurements of cerebral TCA cycle rate in vivo. *Magn Reson Med* 2009; 62: 1641–1645.
21. An L, Li S, Murdoch JB, et al. Detection of glutamate, glutamine, and glutathione by radiofrequency suppression and echo time optimization at 7 tesla. *Magn Reson Med* 2015; 73: 451–458.
22. Bartnik-Olson BL, Ding D, Howe J, et al. Glutamate metabolism in temporal lobe epilepsy as revealed by dynamic proton MRS following the infusion of $[\text{U}^{13}\text{C}]$ glucose. *Epilepsy Res* 2017; 136: 46–53.
23. Dehghani M, Zhang S, Kumaragamage C, et al. Dynamic ^1H -MRS for detection of ^{13}C -labeled glucose metabolism in the human brain at 3T. *Magn Reson Med* 2020; 84: 1140–1151.
24. Pfrommer A, Avdievich NI and Henning A. Four channel transceiver array for functional magnetic resonance spectroscopy in the human visual cortex at 9.4 T 1. In: *Joint Annual Meeting ISMRM-ESMRMB 2014*, 2014, Milano, Italy, p. 1305.
25. Dorst J, Borbath T, Landheer K, et al. Simultaneous detection of metabolite concentration changes, water BOLD signal and pH changes during visual stimulation in the human brain at 9.4T. *J Cereb Blood Flow Metab* 2022; 42: 1104–1119.
26. Avdievich NI, Giapitzakis IA, Pfrommer A, et al. Combination of surface and ‘vertical’ loop elements improves receive performance of a human head transceiver array at 9.4 T. *NMR Biomed* 2018; 31: e3878.
27. Gruetter R and Tkáč I. Field mapping without reference scan using asymmetric echo-planar techniques. *Magn Reson Med* 2000; 43: 319–323.
28. Versluis MJ, Kan HE, Van Buchem MA, et al. Improved signal to noise in proton spectroscopy of the human calf muscle at 7 T using localized B1 calibration. *Magn Reson Med* 2010; 63: 207–211.
29. Mekle R, Mlynárik V, Gambarota G, et al. MR spectroscopy of the human brain with enhanced signal intensity at ultrashort echo times on a clinical platform at 3T and 7T. *Magn Reson Med* 2009; 61: 1279–1285.
30. Giapitzakis I, Shao T, Avdievich N, et al. Metabolite-cycled STEAM and semi-LASER localization for MR spectroscopy of the human brain at 9.4T. *Magn Reson Med* 2018; 79: 1841–1850.
31. Giapitzakis I-A, Avdievich N and Henning A. Characterization of macromolecular baseline of human brain using metabolite cycled semi-LASER at 9.4T. *Magn Reson Med* 2018; 80: 462–473.
32. Cudalbu C, Behar KL and Bhattacharyya PK. Contribution of macromolecules to brain ^1H MR spectra: experts’ consensus recommendations. *NMR Biomed* 2021; 34: 4393.
33. Murali-Manohar S, Borbath T, Wright AM, et al. T2 relaxation times of macromolecules and metabolites in the human brain at 9.4 T. *Magn Reson Med* 2020; 84: 542–558.
34. Provencher SW. Estimation of metabolite concentrations from localized in vivo proton NMR spectra. *Magn Reson Med* 1993; 30: 672–679.
35. Soher BJ, Semanchuk P, Todd D, et al. VeSPA: integrated applications for RF pulse design, spectral simulation and MRS data analysis, <https://scion.duhs.duke.edu/vespa/> (1994, accessed 4 December 2018).
36. Soher BJ. Vespa: versatile simulation pulses and analysis. User code contributions – semi-LASER, <https://scion.duhs.duke.edu/vespa/contrib/wiki/1f03e57e-1d27-4d36-8b31-db9e5e2f73e82013> (accessed 30 July 2019).
37. Giapitzakis I, Borbath T, Murali -Manohar S, et al. Investigation of the influence of macromolecules and spline baseline in the fitting model of human brain spectra at 9.4T. *Magn Reson Med* 2019; 81: 746–758.
38. Govindaraju V, Karl Y and Maudsley AA. Proton NMR chemical shifts and coupling constants for brain metabolites. *NMR Biomed* 2000; 13: 129–153.
39. Govind V, Young K and Maudsley AA. Corrigendum: Proton NMR chemical shifts and coupling constants for brain metabolites. *NMR Biomed* 2015; 28: 923–924.
40. Near J, Evans CJ, Puts NAJ, et al. J -difference editing of gamma-aminobutyric acid (GABA): simulated and experimental multiplet patterns. *Magn Reson Med* 2013; 70: 1183–1191.
41. Marjańska M and Terpstra M. Influence of fitting approaches in LCModel on MRS quantification focusing on age-specific macromolecules and the spline baseline. *NMR Biomed* 2019; 34: 1–9.
42. de Graaf RA. *In vivo NMR spectroscopy principles and techniques*. Chichester, UK: Wiley, 2007.
43. Moreno A, Ross BD and Blüml S. Direct determination of the N-acetyl-L-aspartate synthesis rate in the human brain by ^{13}C MRS and $[\text{1-}^{13}\text{C}]$ glucose infusion. *J Neurochem* 2001; 77: 347–350.
44. Lanz B, Gruetter R and Duarte JMN. Metabolic flux and compartmentation analysis in the brain in vivo. *Front Endocrinol (Lausanne)* 2013; 4: 156–118.
45. Mason GF. CWave: software for the design and analysis of ^{13}C -labeling studies performed in vivo. *Proc Intl Soc Mag Reson Med* 2000; 8: 1870.
46. Mason GF, Gruetter R, Rothman DL, et al. Simultaneous determination of the rates of the TCA cycle, glucose utilization, alpha-Ketoglutarate/glutamate exchange, and glutamine synthesis in human brain by NMR. *J Cereb Blood Flow Metab* 1995; 15: 12–25.
47. Henry PG, Lebon V, Vaufrey F, et al. Decreased TCA cycle rate in the rat brain after acute 3-NP treatment measured by in vivo ^1H - $\{^{13}\text{C}\}$ NMR spectroscopy. *J Neurochem* 2002; 82: 857–866.
48. Watanabe H, Umeda M, Ishihara Y, et al. Human brain glucose metabolism mapping using multislice 2D ^1H - ^{13}C correlation HSQC spectroscopy. *Magn Reson Med* 2000; 43: 525–533.

49. Moreno A, Blüml S, Hwang J-H, et al. Alternative 1-13C glucose infusion protocols for clinical 13C MRS examinations of the brain. *Magn Reson Med* 2001; 46: 39–48.
50. Beckmann N, Fried R, Turkalj I, et al. Noninvasive observation of hepatic glycogen formation in man by 13C MRS after oral and intravenous glucose administration. *Magn Reson Med* 1993; 29: 583–590.
51. Pfeuffer J, Tkáč I, Choi I-Y, et al. Localized in vivo 1H NMR detection of neurotransmitter labeling in rat brain during infusion of [1-13C] D-glucose. *Magn Reson Med* 1999; 41: 1077–1083.
52. Shen J, Petersen KF, Behar KL, et al. Determination of the rate of the glutamate/glutamine cycle in the human brain by in vivo 13 C NMR. *Proc Natl Acad Sci U S A* 1999; 96: 8235–8240.
53. Mason GF, Petersen KF, de Graaf RA, et al. Measurements of the anaplerotic rate in the human cerebral cortex using 13C magnetic resonance spectroscopy and [1-13C] and [2-13C] glucose. *J Neurochem* 2007; 100: 73–86.
54. Lebon V, Petersen KF, Cline GW, et al. Astroglial contribution to brain energy metabolism in humans revealed by 13C nuclear magnetic resonance spectroscopy: elucidation of the dominant pathway for neurotransmitter glutamate repletion and measurement of astrocytic oxidative metabolism. *J Neurosci* 2002; 22: 1523–1531.
55. Gruetter R, Seaquist ER, Kim S, et al. Localized in vivo 13 C-NMR of glutamate metabolism in the human brain: initial results at 4 Tesla. *Dev Neurosci* 1998; 55455: 380–388.
56. Wijnen JP, Van der Graaf M, Scheenen TWJ, et al. In vivo 13C magnetic resonance spectroscopy of a human brain tumor after application of 13C-1-enriched glucose. *Magn Reson Imaging* 2010; 28: 690–697.
57. Murali-Manohar S, Borbath T, Wright AM, et al. Quantification of human brain metabolites using two-dimensional J-resolved metabolite-cycled semiLASER at 9.4 T. In: *2021 ISMRM & SMRT Annual Meeting & Exhibition*, 2021. <https://www.ismrm.org/21/program-files/TeaserSlides/TeasersPresentations/0284-Teaser.html> (accessed June 2021).
58. Ruhm L, Avdievich NI, Ziegs T, et al. Deuterium metabolic imaging in the human brain at 9.4 Tesla with high spatial and temporal resolution. *Neuroimage* 2021; 244: 118639.
59. Pfeuffer J, Tkáč I, Choi I-Y, et al. Detection of [1,6-13 C2]-glucose metabolism in rat brain by in vivo 1H-[13C]-NMR spectroscopy. *Magn Reson Med* 1999; 41: 1077–1083.
60. Gruetter R, Ugurbil K and Seaquist ER. Steady-state cerebral glucose concentrations and transport in the human brain. *J Neurochem* 2002; 70: 397–408.
61. Shestov AA, Valette J, Ugurbil K, et al. On the reliability of 13C metabolic modeling with two-compartment neuronal-glia models. *J Neurosci Res* 2007; 85: 3294–3303.
62. Alper HS. *Systems metabolic engineering: methods and protocols*. Vol. 985, Methods in Molecular Biology, Springer Protocols, Springer, New York, Heidelberg, Dordrecht, London, 2013.
63. Mariager CO, Lindhardt J, Nielsen PM, et al. Fractional perfusion: a simple semi-parametric measure for hyperpolarized 13 C MR. *IEEE Trans Radiat Plasma Med Sci* 2019; 3: 523–527.
64. Gruetter R, Seaquist ER and Ugurbil K. A mathematical model of compartmentalized neurotransmitter metabolism in the human brain. *Am J Physiol Endocrinol Metab* 2001; 281: E100–E112.
65. Pan JW, Stein DT, Telang F, et al. Spectroscopic imaging of glutamate C4 turnover in human brain. *Magn Reson Med* 2000; 44: 673–679.
66. Dehghani MM, Lanz B, Duarte JMN, et al. Refined analysis of brain energy metabolism using in vivo dynamic enrichment of 13C multiplets. *ASN Neuro* 2016; 8: 175909141663234.
67. Henry P-G, Adriany G, Deelchand D, et al. In vivo 13C NMR spectroscopy and metabolic modeling in the brain: a practical perspective. *Magn Reson Imaging* 2006; 24: 527–539.
68. Shen J. Modeling the glutamate-glutamine neurotransmitter cycle. *Front Neuroenergetics* 2013; 5: 1–13.
69. De Graaf RA, Brown PB, Mason GF, et al. Detection of [1,6-13C2]-glucose metabolism in rat brain by in vivo 1H-[13C]-NMR spectroscopy. *Magn Reson Med* 2003; 49: 37–46.